Single Channel Self-Mixing Interferometer Measures Simultaneously Displacement and Tilt and Yaw Angles of a Reflective Target

Silvano Donati, *Life Fellow, IEEE*, Davide Rossi, and Michele Norgia, *Senior Member, IEEE*

***Abstract*— We show that a self-mixing interferometer can supply not only to the usual optical-phase signal cos 2ks(t) of the external reflector displacement s(t), but also the attitude signal P(*a*) because of the dependence of power from the angle *a* between wavevector k and normal n to the target reflective surface. By proper interrogation of P(*a*) along two orthogonal components of tilt and yaw, the two angles can be measured simultaneously, together with the displacement, in a single self-mixing interferometer channel implemented by a single laser diode and monitor photodiode combination.**

***Index Terms* — Optical interferometers, Measurements, Optical feedback, Semiconductor laser diodes.**

I. INTRODUCTION

Self-mixing interferometry (SMI) was introduced about 25 years ago [1], but only in recent years it has attracted much interest because it's a simple yet powerful tool in a variety of applications (see for example Ref.[2] for a review).

Measurements of displacements, vibrations, and related kinematic quantities are the most developed applications of SMI [2-4], and with them we read optical pathlength as a phase $\phi=2ks$, where k is the wavevector and s the target distance, just like in a normal interferometer. But we can also look at other features of the SMI signal, for example amplitude, and develop echo detectors [5,6] good as sensor up to THz frequency [7,8], or at waveform details to measure e.g., index of refraction [9], and linewidth [10] and alpha factor [11,13] of the laser. The still growing areas of application span from engineering [14,15] to biomedical [16,17] to consumer [18].

The theoretical background for SMI operation is also well established and all the experimental findings are nicely explained [4], at increasing level of coverage, by at least three models: (i) the rotating vector model, explaining the amplitude and frequency (AM and FM) modulations generated by the backreflected field, (ii) the 3-mirror model explaining also the waveform switchings due to frequency hopping on the external-cavity modes and, (iii) the Lang-Kobayashi equations for the full coverage of the SMI dynamics, including the case of strong feedback regimes leading to chaos [19].

Yet, rather surprising, another effect always present in the SMI and also due to the backreflection from remote target has been totally ignored till now, that of the *decrease of losses* of the oscillating cavity because of the external reflector contribution. Usually, in an experiment conducted with the basic scheme of SMI (as shown in Fig.1), one looks at the optical power modulation induced by the returning field, described by the signal

$$P(\phi) = P_0 (1+m \cos \phi) \qquad (1)$$

where P_0 is the quiescent power, m is the modulation index, and $\phi=2ks$ is the external pathlength. Actually, the external target affects also the cavity losses of the laser, and makes them decrease at the increase of external reflectivity, with a dependence of quiescent power P_0 from external attenuation A, so that we can re-write Eq.1 in the more general form:

$$P(\phi,A) = P_0(A) (1+m \cos \phi) \qquad (1a)$$

Additionally, using a reflective target, attenuation A is on its turn a function A(*a*) of angle *a* between wavevector k and target surface n, so that we can write:

$$P(\phi,a) = P_0(a) (1+m \cos \phi) \qquad (1b)$$

Note that the dependence on A or *a* adds to the dependence of power amplitude on the modulation index m, because it has a physically different mechanism: the modulation (AM and FM) comes from the phase-dependent vector addition of returning field on the unperturbed in-cavity vector, whereas the backreflection affects losses of the cavity and is a phase-independent effect. Stated in another way, the former is a *coherent* effect, the latter is an *incoherent* one.

Taking advantage of the incoherent dependence of power from the external return, we show that it is possible to

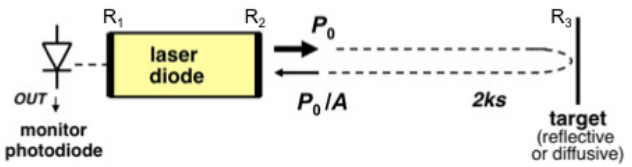

Fig.1 Schematic of a self-mixing interferometer (SMI) using a laser diode to sense the phase shift *2ks* of field returning from an external reflector (or diffuser) at a distance s.

Silvano Donati is with the Department of Industrial and Information Engineering, University of Pavia, v. Ferrata 1, 27100 Pavia, Italy. He is also an Associate of CNR ISASI, "E. Caianiello", Naples (Italy).
M.Norgia and Davide Rossi are with DEIB, Politecnico di Milano.
Corresponding author: silvano.donati@ieee.org

measure, concurrent to the displacement signal ϕ, the angle *a* between $\underline{k}$ and $\underline{n}$, and to resolve it into two orthogonal components, namely tilt and yaw.

The paper is organized as follows: in Section II, we develop the theory of both *ϕ-dependent* modulations and *A-dependent* cavity losses, relative to the power oscillating in the cavity and measured by the rear photodiode (Fig.1).
In Section III we offer some experimental evidence confirming the theory. Then, we turn to consider a reflective target and its dependence of A on alignment angles a_{tilt} and a_{yaw}, and in Section IV we propose the simultaneous measurement of s, a_{tilt} and a_{yaw}, by properly allocating frequency bands to the three signals, in the single output channel of the monitor photodiode output.

II. THEORY

For sake of clarity, let's write explicitly the well-known Lang-Kobayashi (L-K) equations [4,20] for an SMI as:

$$dE/dt = ½ [G_N(N-N_0)-1/\tau_p] E + (K/\tau_{in}) E(t-\tau_{ext})\times \times \cos [\omega_0\tau_{ext} +\phi(t)- \phi(t-\tau_{ext})] \quad (2a)$$

$$d\phi/dt = ½ \alpha\{G_N(N-N_{th})-1/\tau_p\} + (K/\tau_{in}) E(t-\tau_{ext})/E(t)\times \times \sin [\omega_0\tau_{ext} +\phi(t)- \phi(t-\tau_{ext})] \quad (2b)$$

$$dN/dt = J\eta/ed - N/\tau_r - G_N(N-N_0) E^2(t) \quad (2c)$$

where (with values currently used for a FP laser diode):
G_N = modal gain = $8.1\cdot10^{-13}$ $m^3 s^{-1}$,
K = fraction of field coupled into the oscillating mode
N = carrier concentration (m^{-3}),
N_0 at inversion =$1.2\cdot10^{24}$ m^{-3},
N_{th} at threshold = $2.5\cdot10^{24}$ m^{-3},
τ_{ext} =2s/c = round trip time of external cavity
s = distance to external cavity reflector, ϕ= 2ks external optical phaseshift
τ_{in} =$2n_{in}L_{in}/c$ = round trip time of laser cavity = 5 ps,
τ_p = photon lifetime in laser cavity = 2 ps,
τ_r = carrier lifetime = 5 ns,
α = linewidth enhancement factor, (typically 3..6)
$\omega_0 = k_0/c = 2\pi\lambda_0/c$ = unperturbed frequency;
Jη = pumping current density, with
η = internal pumping efficiency
d = active layer thickness = typ. 0.25 μm
V = active volume = typ. 80 $(\mu m)^3$

For slowly varying distance such that $2k[ds(t)/dt]\tau_{ext}<<1$, the phase difference $\phi(t)-\phi(t-\tau_{ext})$ in Eqs.2a-2b is negligible, and then τ_{ext} can be dropped in $E(t-\tau_{ext})$: we take these assumptions for granted in the following.
Factor K in Eqs.2a-2b can be expressed in terms of cavity mirrors reflectivity as:

$$K = \eta_s (1-r_2^2)(r_3/r_2) \quad (3)$$

where η_s is the mode superposition factor, and $r_2=\sqrt{R_2}$ and $r_3=\sqrt{R_3}$ are the field reflectivities of output mirror and target ($r_2^2 \approx 0.35$ for a typical semiconductor cleaved facet).

Now, let's start considering the SMI *ϕ-dependent* injection and calculate the amplitude of the resulting SMI signal P(ϕ). Solving Eq.2b for small K, and after some rearrangements we arrive to the constitutive self-mixing frequency equation, counterpart of Adler's locking equation [4], written in the form [20-22]:

$$\omega t = \omega_0 t - C \sin(\omega t + \text{atan}\,\alpha) \quad (4)$$

In Eq.4 we have introduced the feedback factor C:

$$C=(1+\alpha^2)^{1/2}K\tau_{ext}/\tau_{in} \quad (4a)$$

The C factor determines [4,19-23] the regime of feedback, from *weak feedback* (C<<1) when the waveform F(..) is almost sinusoidal and the amplitude of modulation m is proportional to C, to *moderate feedback* (C≈1) when mode-hopping starts to show up and F(..) exhibits switchings while the amplitude doesn't increase any more, to *strong feedback* (C>>1) when F(..) becomes chaotic with multiple switching per period and the amplitude (peak-to-peak swing) is saturated.

In the case of weak feedback, we can solve the L-K equations (Eqs.2a-2b), on letting K<<1 and calculating field amplitude and phase in the small signal regime as $E=E_0+\Delta E$, and $\omega=d\phi/dt=\omega_0+\Delta\omega$, where E_0 and ω_0 are the quiescent unperturbed values obtained for dE/dt=0, dϕ/dt=0 and K=0. On doing so, we find for small C:

$$\Delta E = [E_0 \kappa C \cos\omega_0\tau_{ext}] / [1+\kappa C \cos\omega_0\tau_{ext}], \quad (5a)$$

where $\kappa= (1+\alpha^2)^{-1/2}\tau_p/\tau_{ext}$ (6)
and

$$\Delta\nu = -(C/\tau_{ext}) \sin(\omega_0\tau_{ext} +\text{atan}\,\alpha)/(1+C\cos\omega_0\tau_{ext}) \quad (7a)$$

Also, for C<<1 we can approximate ΔE and Δν to:

$$\Delta E = E_0 \kappa C \cos\omega_0\tau_{ext}, \quad (5b)$$

$$\Delta\nu = -(C/\tau_{ext}) \sin(\omega_0\tau_{ext}+\text{atan}\,\alpha) \quad (7b)$$

Thus, at weak feedback (C<<1) both AM and FM modulations are sinusoidal and phase-shifted by the difference $\arg(\Delta E)-\arg(\Delta\nu)=\zeta$ of the sine and cosine function, or by $\zeta=\pi/2-\text{atan}\,\alpha$, from Eqs.5b and 7b.

About the output signal found at the photodiode, the photogenerated current $I_{ph}=\sigma P$ is proportional to power P through the spectral sensitivity σ of the photodiode, and so we can limit ourselves to consider power and in particular the signal-dependent part of it, $\Delta P=m P_0$ (as in Eq.1).
Writing $P_0+\Delta P = <[E_0+\Delta E]^2>$ and using Eq.5b we get, for weak feedback (C<<1):

$$\Delta P = 2 E_0^2 \kappa C ½ = P_0 K \tau_p/\tau_{in} \quad (8a)$$

whereas for strong feedback (when C>>1) Eqs.5 and 7 are no more valid and we shall solve numerically the L-K equations (Eq.2a-2b). Doing so, we find [14,15] that the signal saturates at the value corresponding to $C\approx (1+\alpha^2)^{1/2}$ in Eq.8a, so that:

$$\Delta P \approx E_0^2 \kappa(1+\alpha^2)^{1/2} = P_0 \tau_p/\tau_{ext} \quad (8b)$$

In conclusion, the SMI *ϕ-dependent* signal is governed by the C parameter both in shape (the F function) and amplitude (the modulation index m): at weak feedback F is about a sine wave and $m \approx \kappa C$, whereas at moderate and strong feedback function F is a distorted sine (and then chaotic) waveform and the modulation index is $m \approx \tau_p/\tau_{ext} \approx$ const.

For a semiconductor laser, with the target placed at a distance s=60mm, we get from Eq.8b a saturation at m≈0.01, independent from external mirror reflectivity, in good agreement with experimental observation.

Second, let's now consider the *A-dependent* cavity losses induced by the external reflector.

The reflectivity r_3 of the external target of course affects also the factor K of the coherent injected term (Eq.2a) already taken into account, but also the cavity losses summarized by the photon lifetime in the laser cavity τ_p. With a simple loop gain argument, by noting that the rate of decay of power inside the cavity is given by the inverse of the loss per transit time, it is easy to see that for an unperturbed cavity formed by mirrors with (power) reflectivity $R_1=r_1^2$ and $R_2= r_2^2$, and with $R_3=0$, the unperturbed photon lifetime τ_{p0} is found as:

$$\tau_{p0} = \tau_{in} [-\ln (R_1 R_2)]^{-1} \qquad (9a)$$

whereas, on adding the third mirror with (power) reflectivity R_3, we have also the external cavity formed by R_2 and R_3 and the (perturbed) photon lifetime is increased to:

$$\tau_p \approx \tau_{in} \{-\ln R_1[R_2+(1-R_2)^2R_3/(1-R_3R_2)]\}^{-1} \qquad (9b)$$

or, the effective reflectivity R_2^* of the output mirror is changed to:

$$R_2^*=R_2+(1-R_2)^2R_3/(1-R_3R_2), \qquad (9c)$$

where term $(1-R_2)^2R_3$ is the contribution returning from target R_3 after a double transmission through R_2, and $(1-R_3R_2)$ accounts for multiple reflections between R_3 and R_2.

Photon lifetime affects two quantities readily measured from the static P-I characteristics of the laser: (i) the threshold current J_{th} and (ii) the slope efficiency $S=P/(J- J_{th})$.

To find their dependence, we solve Eq.2c for E^2 in the stationary conditions dN/dt=0 and above threshold, where the term $(N-N_{th})/\tau_r$ can be assumed much smaller than $(J-J_{th})/ed$ (a condition called pinning of N). Noting also, from Eq.2a, that $G(N-N_0)=1/\tau_p$, we get:

$$E^2/\tau_p= (J-J_{th})\,\eta/ed - (N-N_{th})/\tau_r \approx (J-J_{th})\,\eta/ed \qquad (10a)$$

and introducing $P=E^2$ in Eq.10a, the slope efficiency S is found to be directly proportional to photon lifetime τ_p:

$$S = P/(J-J_{th})= \tau_p\eta/ed \qquad (10b)$$

If we start from $R_3=0$ ($\tau_p=\tau_{p0}$) at which $S_0=\tau_{p0}\eta/ed$ and then let R_3 increase so that $\tau_p>\tau_{p0}$, the slope S will vary as $\Delta S=(\tau_p-\tau_{p0})\,\eta/ed=\Delta\tau_p\,\eta/ed$, and then the relative slope $\Delta S/S_0$ is:

$$\Delta S/S_0 = \Delta\tau_p/\tau_{p0} \qquad (10c)$$

About threshold J_{th}, from Eqs.2c we have $J_0/ed=N_0/\tau_r$ and therefore also $J_{th}/ed=N_{th}/\tau_r$. Moreover, from Eq.1c we get $N_{th}= N_0+1/G\tau_p$ and $J_{th}/J_0=N_{th}/N_0=1+1/GN_0\tau_p$.

Now, starting from a value J_{th0} of unperturbed threshold (i.e., for $R_3=0$) at which the photon lifetime is τ_{p0}, and going to a perturbed condition ($R_3\neq0$) with a new value τ_p, we can compute the threshold variation $\Delta T=J_{th}-J_{th0}$, and then the relative threshold variation $\Delta T/T_0=(J_{th}-J_{th0})/J_{th0}$ as a function of $\Delta\tau_p=\tau_p-\tau_{p0}$. The result reads:

$$\Delta T/T_0=(J_{th}-J_{th0})/J_{th0} = [1/GN_0\tau_p -1/GN_0\tau_{p0}]\,/(1+1/GN_0\tau_{p0})$$
$$= (\tau_{p0}-\tau_p)/\{\tau_p[1+GN_0\tau_{p0}]\} = -(\Delta\tau_p/\tau_p)/[1+GN_0\tau_{p0}] \qquad (11)$$
$$\approx -(\Delta\tau_p/\tau_{p0})/[1+GN_0\tau_{p0}] \quad \text{for } \tau_p\approx\tau_{p0} \qquad (11a)$$

As a conclusion of the analysis, slope and threshold are both affected by changes in mirror reflectivity R_3 because of the dependence on photon lifetime τ_p given by Eq.9b.

When the external mirror reflectivity R_3 is changed, lifetime τ_p varies according to Eq.9b, and from Eq.10b we see that slope variations are equal to lifetime variations $\Delta\tau_p/\tau_{p0}$; moreover, from Eq.11, we see that threshold variations are just the lifetime variations $\Delta\tau_p/\tau_{p0}$ scaled by the factor $-[1+GN_0\tau_{p0}]$, when $\tau_p\approx\tau_{p0}$ (or, R_3 is small).

III. Experimental Validation

We have tested the validity of the model using a VCSEL diode, model PH85-F1P1S2-KC of Optowell Co., emitting 8 mW at 850 nm at a nominal drive current of 20 mA.

Reason for choosing a VCSEL is that the spot is reasonably circular and no asymmetry is introduced in the tilt and yaw measurement; however we also tested FP-laser and found they are described equally well by the model.

We used the simple feedback scheme of Fig.1, with a reflecting target placed at a distance of 60-mm and properly

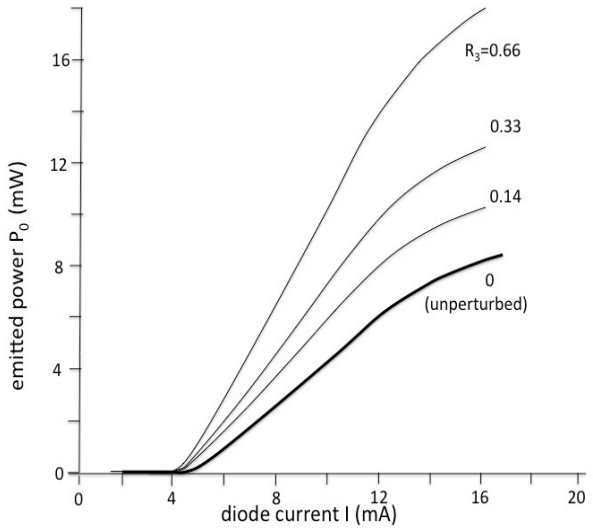

Fig.2 Experimental power-current curves for our VCSEL emitting at 850 nm. Thick line is the unperturbed case (R_3 =0), thin lines are the power emitted at three values of target reflectivity R_3.

aligned so as to maximize the return into the laser cavity. The reflecting targets were flats of: sapphire (R_3=0.14), Silicon (R_3=0.33) and Nickel (R_3=0.66), all with the back surface blackened to avoid spurious contributions.

The power-current curve dramatically depends on the target reflectivity, more than doubling for R_3=0.66 at I=16 mA respect to the unperturbed condition R_3=0, see Fig.2.

The slope of the power-current curve also increases with R_3, and, in the moderate current range where slope S=P/I is almost constant, it supplies the experimental value of $\Delta S/S_0 = \Delta\tau_p/\tau_{p0}$.

Also, by drawing the tangent to the initial part of the P-I curve and extrapolating it linearly to zero power we could easily measure experimentally the relative variation of threshold, $-\Delta T/T_0$.

Experimental data we measured for the VCSEL PH85-F1P1S2-KC with external reflector are collected in Table I.

Table I

reflectivity R_3	0	0.14	0.33	0.66
threshold variation $\Delta S/S_0$ (%)	0	2.2	3.5	9.2
slope variation $-\Delta T/T_0$ (%)	0	9	15	48
slope-to-threshold ratio	-	4.1	4.3	5.1

By combining Eqs.10c and 11, we can calculate the ratio of relative slope-to-threshold variations with reflectivity R_3. For small perturbation ($\tau_p \approx \tau_{p0}$ or small R_3) we get:

$$-(\Delta T/T_0)/(\Delta S/S_0) = 1+GN_0\tau_{p0} \qquad (12)$$

For a VCSEL, the commonly assumed values [24] of gain g_N and of carrier concentration at transparency N_t are: $g_N = 2.5\times 10^{-16}$ cm^2 and $N_{th}=1.3\times10^{18}$ cm^{-3}. By converting these quantities to our parameters G and N_0 of Eqs.2, we get: $G = c\, g_N = 2.5\ 10^{-16}\times 3\ 10^{10}$ cm^3/s$=7.5\ 10^{-12}$ m^3/s and $N_0 = N_t = 1.3\ 10^{24}$ cm^{-3}.

Consequently, factor $[1+GN_0\tau_{p0}]$ in Eq.12 is evaluated as $1+9.75\ \tau_{p0}$, where τ_{p0} is in ps.

Then, we can start by matching the experimental result of slope-to-threshold ratio at small R_3, that is $-(\Delta T/T_0)/(\Delta S/S_0)$ =4.1 in Table I, and to do so we need τ_{p0}=(4.1-1)/9.75=0.318 ps. This value corresponds, in a L=10 μm VCSEL cavity with τ_{in}=0.2-ps, to a mirror reflectivity product (following Eq.9a)

$$R_1R_2 = \exp -\tau_{in}/\tau_{p0} = 0.533 \qquad (13)$$

As the manufacturer did not provide data about mirror reflectivity of our laser diode, we looked for best match of experimental data to theory. On taking R_1=0.90 and R_2 =0.59 (i.e., a back mirror with high reflectance) we get a reasonable good fit with experimental data, as shown in Fig.3 (full line), where $-\Delta T/T$ and $\Delta S/S$ from Eqs.10c and 11 are plotted.

On the other side, should we assume the cavity loss is equally shared by the two mirrors, i.e., $R_1=R_2$ =0.73, the match becomes appreciably worsened (Fig.3, dotted lines).

One reason for the limited accuracy of the match is that the extra contribution in Eq.9c makes the decay rate governed by a double-time constant regime, different from the simple exponential assumed to derive Eqs.9b and 13.

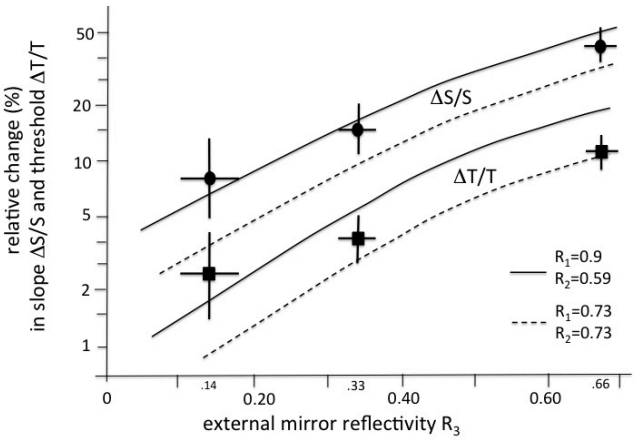

Fig.3 Match of theoretical and experimental values of slope ΔS/S (dots) and threshold ΔT/T (squares) as a function of external mirror reflectivity. Full lines represent the best matching, found for a high reflectance back mirror (R_1=0.9) and R_2=0.59 as derived from the τ_{p0} value, ruling out that the two laser mirrors are same reflectivity $R_1 = R_2$=0.73 (dotted lines).

Another reason is the eventual existence, in some lasers, of a leak contribution due to backreflected light passing around the laser chip and reaching directly to the rear monitor photodiode. This stray contribution makes the apparent laser power increase, and should be subtracted from the true photodetected current I_{ph} due to the backface-emitted power reaching the photodiode. The existence of a stray photocurrent is revealed by comparing the variations of photodiode current and of voltage V_{LD} across the laser junction, this last being obviously unaffected by the stray contribution. For our VCSEL chip having an area of 500x500μm^2, the stray contribution was expected to be

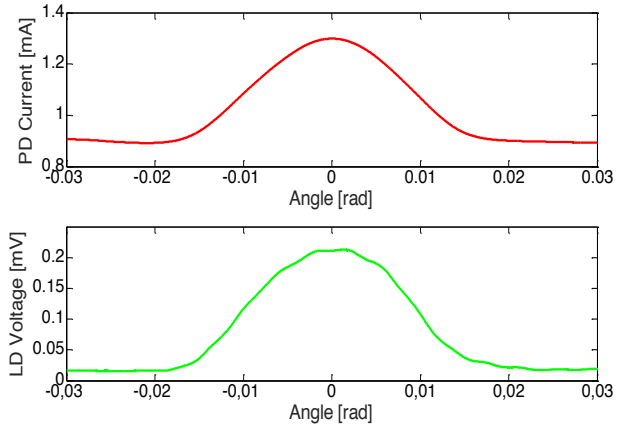

Fig.4 The P(*a*) dependence on angle *a*, as measured by the photodetected current I_{ph} at the monitor photodiode (top) and by the diode voltage V_{LD} (bottom) are quite the same and confirm that no appreciable leakage contribution is collected. Setup data: 2H=120 mm, w_0=1.5 mm.

negligible in our working condition of well-collimated output beam, because the returning beam retraces the output rays and isn't spread enough to escape the chip.

This conjecture is confirmed by the nearly coincident trend of detected photocurrent I_{ph} and diode voltage V_{LD} reported in Fig.4. Incidentally, it is worth noting that, if the VCSEL diode hasn't a rear monitor photodiode, the measurement can be anyway carried out by using the diode voltage as the sensing signal (albeit with a reduced SNR respect to the I_{ph}, as indicated by the small ripple in Fig.4, bottom).

IV. Instrumental Development

The angle dependence of power P(a) can be exploited to measure angle a between wavevector $\underline{k}$ of output beam and the normal $\underline{n}$ to the target surface. In particular, we can measure tilt ψ and yaw θ angles of the reflective target surface (see Fig.5). This measurement can be carried out simultaneously to the SMI measurement of displacement s, as detailed below.

Of course, different from the usual operation of an SMI, where for measuring displacements we can also employ a *diffusing* target, we now shall restrict operation to *reflective* target to read the angle signal.

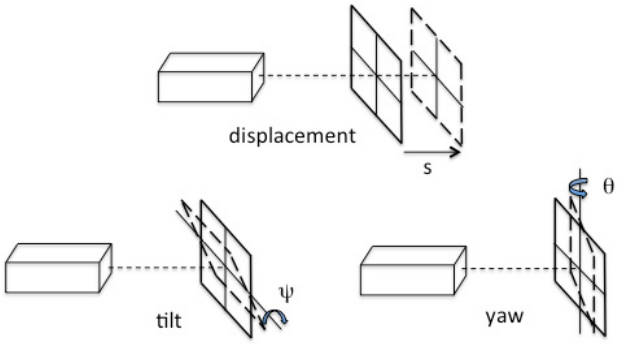

Fig.5 Three quantities describing target movement can be measured simultaneously from the P(ϕ,A) signal (see Eq.1a): displacement s as in a normal self-mixing interferometer, and the angles ψ and θ of tilt and yaw of the target surface, here drawn separately for clarity.

When the reflective target is moved of an angle a from alignment of its normal $\underline{n}$ to wavevector $\underline{k}$, the superposition of retuning beam and unperturbed mode distribution inside the cavity results in a dependence of emitted power P(a) found as [25]:

$$P_0(a) = P_0 + P_{00} \exp -(2aH)^2/w_0^2 \qquad (14)$$

where $a=[\psi^2+\theta^2]^{1/2}$ is the composite tilt plus yaw angle, H is the laser-to-target distance, and w_0 is the spot size of the beam projected by the laser onto the target, assumed Gaussian and nearly constant because of the collimation provided by the objective lens placed at the laser output.

Eq.14 applies for a circular spot size like the one emitted by our VCSEL; if a FP-laser diode is used, Eq.14 should be duplicated for the two spot sizes w_{0X} and w_{0Y} along axes X and Y, the axes that conveniently will be made coincident with the reference system of tilt and yaw (Fig.5) measurement.

The Gaussian shape of response of power P(a) as a function of angle is fairly well matched (within, say a few percent) [25] provided the laser emits a clean spatial fundamental mode and care is exercised that the beam doesn't suffer spurious reflections inside the optical elements.

To transform the Gaussian dependence to an almost-linear one, we use the following well-known technique. A small modulation Δa (say $\Delta a=\Delta a_0 \cos \omega_m t$) is superposed to the angle a to be measured, so that the small increment Δa is multiplied by the *derivative* of the dependence (14), or:

$$P_0(a+\Delta a) = P_0(a)+[dP_0(a)/da]\,\Delta a \qquad (15a)$$

$$= P_0(a)+P_0(a)\,2a\Delta a\,(2H)^2/w_0^2 \qquad (15b)$$

Thereafter, we detect the corresponding signal by a lock-in (or phase sensitive) amplifier centered at ω_m. The lock-in output is then the second term at the right hand side of Eq.15b, that is, a linear dependence multiplied by a Gaussian, as already shown in Refs.[25, 26].

The useful, almost-linear range of measurement is about $a\approx\pm(1.0\text{-}1.6)w_0/H$, before the signal reaches a saturation and bends back (see Fig.7 below and Fig.3 of Ref.25). In our setup, with w_0=1.5-mm and H=80-mm, the useful linear range was about ±45 mrad (or ±2.5 deg).

We can do better however, if we compute the *relative derivative* S(a) of the power versus angle. We do so by dividing the synchronously detected signal (second term in Eq.15b) by signal (dc) component (first term in Eq.15b), thus obtaining:

$$S(a)= [dP_0(a)/da] / P_0(a) = a\,[8H^2/w_0^2] \qquad (15c)$$

This a truly linear dependence versus angle, which is extended up to the range where signal $P_0(a)$ becomes too small (and SNR is impaired), e.g. $a \approx\pm 3\text{-}4w_0/H$ typically.

The $P_0(a)$ signal carrying the angle information is just the baseline (or mean level) of the self-mixing signal we find at the monitor photodiode output (Fig.1), whereas the displacement signal is the a.c. component impressed on it, one that is easily separated by filtering. To get the linearized signal S(a), we apply a small-amplitude variation Δa to the angle, and look to the resulting relative power variation (Eqs.15b and c). Conveniently, we will apply Δa as an a.c. modulation, that is $\Delta a= \Delta a_0 \cos \omega_m t$, and then by a lock-in amplifier working at the modulation frequency ω_m we will be able to retrieve $\Delta P_0(a)$ [and S(a)], without significantly occupying the spectrum of the self-mix signal, one let available for the displacement component.

Thus, with this scheme we can measure simultaneously the displacement and an angle.

Next step, we can also make a *duplex* angle measurement, simply by modulating one angle by cos $\omega_m t$, and the other by sin $\omega_m t$, thus generating two orthogonal components that will be separated by the two-channel operation (phase and quadrature) of the lock-in amplifier fed by the photodiode output signal. Thanks to the duplex, we can accommodate

simultaneous tilt and yaw angle measurements as well as the displacement measurement in a single self-mix signal.
In the following, we outline the implementation of the idea and provide some experimental evidence.

The angle modulation is readily obtained, as already reported in previous papers [25-27], by mounting the objective collimating lens (we used a 5-mm diameter, 0.5 NA, commercial lens) in a holder with two small piezoceramic chips on either side of a diameter, along X and Y axes, as shown in Fig.6. Note the that, different from another possible control developed in Ref.[28], focus is not altered in this arrangement.

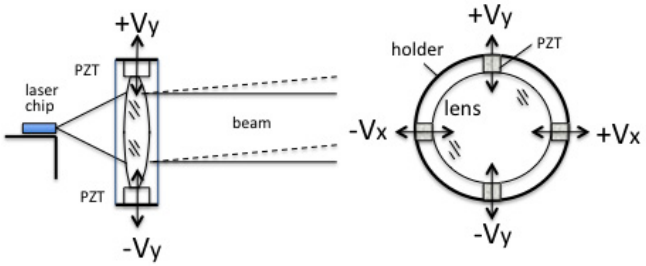

Fig.6 Mounting the objective lens on PZT piezo drivers, arranged along the X and Y axis and driven in push-pull, to modulate tilt θ and yaw ψ angles of the beam.

The piezo are driven in push-pull with $+V_d$ and $-V_d$ to impart a transversal movement without exerting significant stress on the lens. With typical piezo of 1-mm by side, the transversal movement was Δ_{tm}=2μm, corresponding to a modulation of angle $\Delta a_{mod}= \Delta_{tm}/F=2\ 10^{-6}/5\ 10^{-3}$ =2.2 mr, more than enough in amplitude respect to the 50-mr full range, and adequate for a good SNR of the measurement.

To ensure the X and Y channel are independent, we might have also used different modulation frequencies for the two driving signals. In this case, however, the band occupancy is doubled. It's better to let the signal be an orthogonal pair at the same frequency (as already shown in Ref.[25]), that is:

$$V_{dX} = V_0 \cos 2\pi f_m t, \qquad V_{dY} = V_0 \sin 2\pi f_m t \qquad (16)$$

So, tilt $a_{tilt}=\psi$ and yaw $a_{yaw}=\theta$ angles are modulated as:

$$\Delta\psi = \Delta\psi_0 \cos 2\pi f_m t, \qquad \Delta\theta = \Delta\theta_0 \sin 2\pi f_m t \qquad (16a)$$

Upon synchronous detection of the photocurrent signal $I_{ph}=\sigma P(a+\Delta a)$ (Eq.15) the phase V_P and quadrature V_Q outputs of the lock-in provide simultaneously the tilt and yaw signals:

$$V_P = \langle V_{dX}\, P_0(a+\Delta a)\rangle = V_0\, P_0(a)\, \psi\Delta\psi_0 (2H)^2/w_0^2$$

$$V_Q = \langle V_{dY}\, P_0(a+\Delta a)\rangle = V_0\, P_0(a)\, \theta\Delta\theta_0\, (2H)^2/w_0^2 \qquad (17)$$

[note that the displacement signal cos ϕ (Eq.1) is averaged out to zero in Eq.17, except for a narrow-band component at frequency f_m]. Drive frequency f_m is chosen in the low-audio range (e.g., $\omega_m/2\pi$=20-Hz) to minimize cross-talk with the displacement signal. Amplitude of the piezo driver is in the range of 5-10 V. The drive waveforms (sine/cosine) are also used as the references of the lock-in for duplex demodulation of ψ and θ.

A notch filter is used to remove the modulation carrier ω_m from the photodetected current, to leave a clean self-mixing signal (the one of the normal SMI) carrying the ϕ=2ks information. The complementary signal, that is the bandpass filtered SMI, is the angle-dependent signal sent to the lock-in.

To test the linearity of the angle measurement response, a measurement was carried out by mounting the target (a flat with R=0.33 reflectivity) on a rotatable platform with arc-minute resolution, and then comparing the lock-in output to platform readout.
No appreciable difference was found between tilt and yaw measurements, and a good linear trend with error less than 2% was found up to about ±6 mrad, and less than 10% up to about 15 mrad (full lines in Fig.7) for a single measurement lasting 50-ms.
These results are obtained with the relative derivative algorithm (Eq.15c), whereas the plain derivative measurement (dotted lines in Fig.7) deviates much earlier, at about 3.5 mrad for a 5% linearity error.
The error bars in Fig.7 correspond to one standard deviation, estimated over 70 repeated measurements. The angle error is limited to 0.2-mrad for the range ±6 mrad, and is mainly due to electrical disturbances. By averaging on several (N=100) samples, the error drops to 12-μr, comparable to values found in Ref. [25].

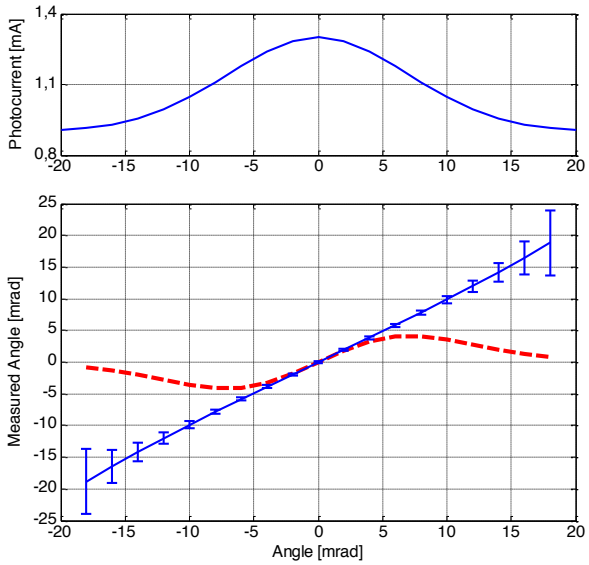

Fig.7 Top diagram: the P(*a*) Gaussian response, for a setup with 2H=190 mm, w_0=1.5 mm. Bottom diagram: experimental measurement of the angle (tilt or yaw) response of the self-mix P(*a*) signal obtained by: (i) piezo modulation of the beam aim (Eq.15b) - dashed line, and (ii) using the relative derivative linearization of (Eq.15c) - full line. Note the improvement of the linear dynamic range obtained by the relative derivative algorithm, only limited by the worsening of the SNR (i.e., the increasing size of the bars).

Duplex angle measurement

To illustrate the waveforms in a simultaneous measurement of displacement and angles, we used the jig shown in Fig.8. It consists of an optical flat (R=0.33) pivoted at one fixed end-

point along the edge, and driven by a loudspeaker at the opposite end of the edge.

First case, we switched off the piezo scan of objective lens, and by the loudspeaker delivered a periodic tilt θ toward the observer, as well as a position-dependent displacement s. The displacement is a maximum at P2 (Fig.8) and damps out to zero at P1, whereas the tilt angle θ is constant all over the target.

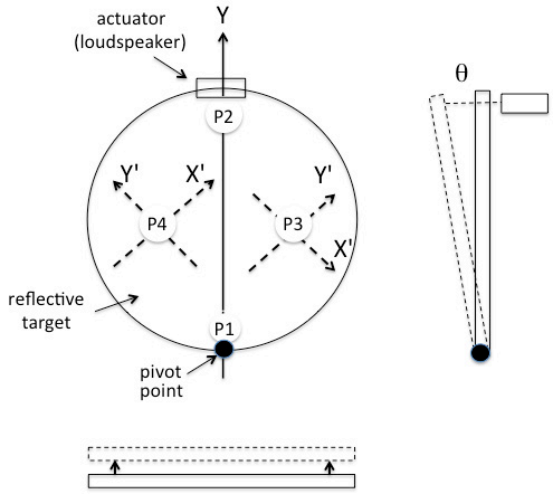

Fig.8 Experimental jig to develop illustrative time-varying SMI and angle signals.

In Fig.9 we report the corresponding experimental SMI waveforms, detected at P1 and P2. At P1 (the pivot point) the signal is pure angle, whereas at P2 the signal has a large cos ϕ displacement component superposed to the angle θ signal (visible as a ripple).

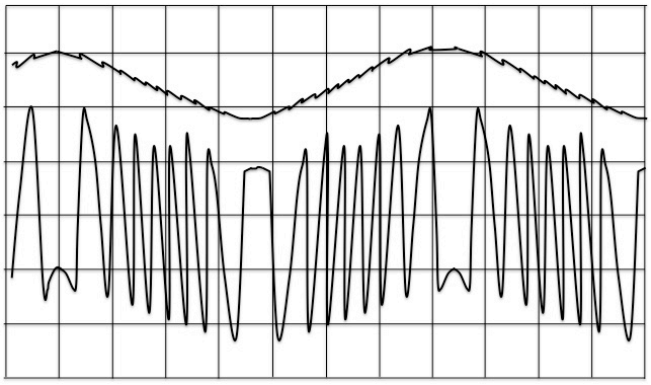

Fig.9 Experimental waveforms of self-mix signals (drawn from actual oscilloscope traces). Top: an almost pure angle *a* signal is found at point P1 of Fig.8, whereas at P2 (bottom) the main contribution is the displacement signal *2ks* and the angle component is revealed by the underlying ripple.

Amplitude of displacement was about 5 μm, angle about 1 mrad, and the C factor was adjusted around unity by adding a x20 attenuation in the optical path.

Second case, we turned the target by a constant (d.c.) amount θ_0=2-mr, and switched-on the piezo drives. By rotating of ±45 deg the X'-Y' axes of the piezo (Fig.8), we develop (simulated) tilt $\theta_{X'}$ and yaw $\theta_{Y'}$ angles respect to axes of analysis defined by the piezo. Projecting θ_0 on the X'-Y' axes, we then have $\theta_{Y'}=-\theta_{X'}=(1/\sqrt{2})\,\theta_0$ at point P3 and $\theta_{Y'}=\theta_{X'}=(1/\sqrt{2})\,\theta_0$ at point P4.

Thus, the complete angle signal is proportional to θ_0 $(\cos 2\pi f_m t \pm \sin 2\pi f_m t) = \theta_0 \sin(2\pi f_m t \pm 45°)$, with the + sign at P4 and the - sign at P3. The corresponding waveforms obtained after bandpass filtering at $f=f_m$ are reported in Fig.10 and show the expected 90-deg phaseshift of P3 respect to P4. Also, using Eq.7, we find the correct values of the demodulated (angle) signals, that is: $V_P = V_0\,\theta_{Y'}$ and $V_Q = -V_0\,\theta_{X'}$ at point P3, and $V_P = V_0\,\theta_{Y'}$ and $V_Q = V_0\,\theta_{X'}$ at point P4.

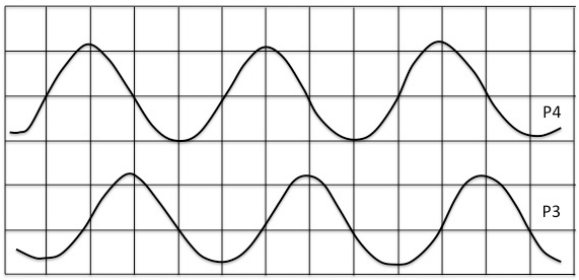

Fig.10 Experimental waveforms (drawn from actual oscilloscope traces) of angles detected along the X' Y' axes (points P3 and P4 in Fig.8) with tilt at +45 deg (top) and -45 deg (bottom), after having removed the displacement signal by bandpass filtering; the waveforms are 90-deg out of phase as expected.

V. CONCLUSIONS

By using the incoherent effect of power dependence upon the alignment angle of a reflective target, together with the usual coherent self-mixing dependence on external pathlength, we have demonstrated that the SMI can perform the simultaneous measurement of displacement and angles, tilt and yaw, taking advantage of two orthogonal modulations of the beam aim.

VI. ACKNOWLEDGEMENTS

Authors wish to thank T.Tambosso and G.Martini for their participation in the early stage of this work.

REFERENCES

[1] S. Donati, "Laser Interferometry by Induced Modulation of the Cavity Field", *Journal Appl. Phys.*, vol.49 (1978), pp.495-497.

[2] S. Donati: "Developing Self-Mixing Interferometry for Instrumentation and Measurements" *Laser Photonics Rev*. vol.6 (2012), pp. 393–417 (DOI) 10.1002/ lpor.201100002.

[3] G.Giuliani, M. Norgia, S. Donati, T.Bosch: 'Laser Diode Self-Mixing Technique for Sensing Applications', *J. of Optics A,* vol.4, (2002), pp.S283-S294.

[4] S. Donati: "*Electrooptical Instrumentation*", Prentice Hall, Upper Saddle River, N.J., 2004.

[5] S. Donati: "Responsivity and Noise of Self-Mixing Photodetection Schemes", *IEEE Journal Quantum El*., vol.47, 2011, pp.1428-1433.

[6] S. Donati, M. Sorel: "A Phase-Modulated Feedback Method for Testing Optical Isolators Assembled in the Laser Package", *IEEE Photonics Techn. Lett.*, vol. 8 (1996), pp. 405-408.

[7] P.Dean, Y.L.Lim, A.Valavanis, R.Kleise, M.Nikolic, S.P.Khanna, M.Lachab, D.Indjin, Z.Ikonic, P.Harrison, A.D.Rakic, E.H.Lindfield, G.Davies: "Terahertz Imaging through Self-Mixing in a Quantum Cascade Laser", *Opt. Lett.* vol.36, pp.2587-2589 (2011).

[8] P.Dean, A.Valavanis, J.Keeley, K.Berting, Y.L.Lim, R.Alhathool, S.Chowdury, T.Taimre, L.H.Li, D.Indjin, S.Wilson, A.D.Rakic, E.H.Linfield and A.G.Davies: "Coherent three-dimensional terahertz imaging through self-mixing in a quantum cascade laser" *Appl. Phys. Lett.,* vol.103 (2013) DOI 181112.

[9] M.Fathi, S.Donati: "Thickness Measurement of Transparent Plates by a Self-Mix Interferometer", *Optics Letters*, vol.35, 2010, pp.1844-46.

[10] G.Giuliani, M. Norgia: 'Laser Diode Linewidth Measurement by means of Self-Mixing Interferometry', IEEE Photonics Technology Letters, vol.PTL-12 pp.1028-1030. (2000)

[11] Y. Yu, G. Giuliani, S. Donati, "Measurement of the Linewidth Enhancement Factor of Semiconductor Lasers by Self-Mixing Effect", *IEEE Photon. Technol. Lett*., vol.16, pp. 990-992 (2004).

[12] J.Xi, Y.Yu, J.F.Chicaro and T.Bosch: "Estimating the parameters of Semiconductor lasers Based on Weak Optical Feedback Self-Mixing Interferometry" *IEEE J. Quant. Electr.,* vol.41 (2005), pp.1058-1064.

[13] R.Kliese, T.Taimre, A.Bakar, Y.L.Lim, K.Bertling, M.Nikolic, J.Perchoux, T.Bosch and A.D.Rakic: "Solving Self-mixing Equations for Arbitrary Feedback Level: A Concise Algorithm", *Appl. Optics* vol.53 (2014), pp.3723-3736.

[14] S. Donati, V. Annovazzi Lodi, S. Merlo, and M. Norgia, "Measurements of MEMS Mechanical parameters by Injection Interferometry", *Proc. IEEE-LEOS Conference on Optical MEMS*, Kawai, HI, 21-24 Aug.2000, pp.89-90, see also: *IEEE Transaction on Mechatronics*, vol.6 (2001), pp.1-6.

[15] R. Atashkooei, J.C Urresty, S. Royo, J.R.Riba and L.Romeral: "Runout tracking in electrical motors using self-mixing interferometry", *IEEE Trans. Mechatronics*, vol.19 (2014), pp. 184-190.

[16] S. Donati, M.Norgia: "Self-mixing Interferometry for Biomedical Signals Sensing" (invited paper), *IEEE Journal Select. Topics Quantum El*. vol.20, 2014, DOI 10.1109/JSTQE.2013.2270279

[17] A.Arasanz, F.J.Azcona, S.Royo, A.Jha and J.Padellorens: "A new method for the acquisition of arterial pulse wave using self-mixing interferometry", *Opt. and Laser Techn*. vol.63 (2014), pp.98-104

[18] Philips NV (Eindhoven): "Twin Eye Laser Sensor" (SMI integrated chip), see http://www.photonics.philips.com/application-areas/sensing (2011)

[19] S.Donati, M.Fathi: "Transition from Short-to-Long Cavity and from Self-Mixing to Chaos in a Delayed Optical Feedback Laser", *IEEE Journal Quantum El*. vol.48, 2012 pp.1352-1359.

[20] R. Lang and K. Kobayashi, "External Optical Feedback Effects on Semiconductor Injection Laser Properties", *IEEE J. Quant. Electr.*, vol.QE-16 (1980), pp.347-355.

[21] Y.Yu, J. Xi and J.F.Chicaro: "Measuring the feedback parameter of a semiconductor laser with external optical feedback" *Optics Express* vol.19 (2011), pp.9582-9593

[22] S. Donati, S. Merlo: "Applications of diode laser feedback interferometry", Invited Paper, *J. of Optics A*, vol.29 (May 1998) pp.156-161.

[23] Y.Yu and J. Xi: "Influence of external optical feedback on the alpha factor of semiconductor lasers" *Opt. Lett.* vol.38 (2013) pp.1871-1873.

[24] S.F.Yu: "Analysis and Design of VCSEL",Wiley Interscience, New York 2003.

[25] S.Donati, T.Tambosso, R.-H.Horng: "Curvature of Substrates is Measured by means of a Self-Mixing Scheme" *IEEE Photonics Techn. Lett.,*vol.26, 2014, pp. 2170-2174. DOI 10.1109.

[26] G. Giuliani, S.Donati, M. Passerini, T. Bosch: 'Angle Measurement by Injection Detection Interferometry in a Laser Diode', *Optical Engineering*, vol.40, (2001), pp.95-99.

[27] M. Norgia, S.Donati, D. d'Alessandro: "Interferometric Measurements of Displacement on a Diffusing Target by a Speckle-Tracking Technique", *IEEE J. Quant. Electr.*, vol. QE-37 (2001), pp.800-806.

[28] U.Zabit, R.Atashkooei, T.Bosch, S.Royo, F.Bony and A.D.Rakic: "Adaptive Self-Mixing Vibrometer based on a Liquid Lens" *Opt. Lett.* vol.35 (2010), pp.1278-1280.

[29] M. Norgia, S. Donati, "A Displacement-Measuring Instrument Utilizing Self-Mixing Interferometry", *IEEE Transactions on Instrument. and Meas.,* vol. IM-52, no.6 (2003), pp. 1765-1770.